Temperature dependence of electron beam induced current contrast of deformation-induced defects in silicon

2004 J. Phys.: Condens. Matter 16 S201

(http://iopscience.iop.org/0953-8984/16/2/023)

INSTITUTE OF PHYSICS PUBLISHING JOURNAL OF PHYSICS: CONDENSED MATTER

J. Phys.: Condens. Matter **16** (2004) S201–S205 PII: S0953-8984(04)66980-3

Temperature dependence of electron beam induced current contrast of deformation-induced defects in silicon

O V Feklisova[1], E B Yakimov[1], N Yarykin[1] and B Pichaud[2]

[1] Institute of Microelectronics Technology and High Purity Materials RAS, 142432 Chernogolovka, Russia
[2] Laboratoire TECSEN UMR6122, University Aix-Marseille III, 13397 Marseille Cedex 20, France

Received 31 July 2003
Published 22 December 2003
Online at stacks.iop.org/JPhysCM/16/S201 (DOI: 10.1088/0953-8984/16/2/023)

Abstract
Electron beam induced current (EBIC) investigations of plastically deformed silicon in the temperature range from 90 K to 300 K were carried out. It is found that the dislocation trails left behind moving dislocations are the main defects revealed by the EBIC in crystals deformed in clean conditions. With an increase of the contamination level, the dislocation contrast in p-type samples increases. It is observed that the EBIC contrasts of both dislocations and dislocation trails increase with cooling in p-type silicon, while in n-type samples the EBIC contrasts exhibit the opposite trends for both defects.

1. Introduction

The strong interest in the electronic properties of 1D objects has stimulated extensive investigations of dislocated silicon during the last four decades (for recent reviews see [1, 2]). However, the intrinsic dislocation properties have not been established until now. To a great extent this was determined by the strong interaction of dislocations with impurities that could lead to the reconstruction of the dislocation core and to the formation of electrically active defects in the Cottrell atmosphere around the dislocations. Moreover, other point and/or extended defects are formed during plastic deformation near the slip plane swept by the moving dislocation, forming the dislocation trail [3–5]. The defects in the trail are electrically active [6–9] and can strongly affect the macroscopic electrical properties of the crystals. To distinguish between the contributions from different defects, their electrical properties should be studied separately. One of the most suitable techniques for such investigations is the EBIC mode of a scanning electron microscope, which provides the lateral resolution to study different defects in the same sample.

It is shown that dependences of the EBIC contrast on the electron beam current measured at different temperatures supply a wealth of information about the electronic structure of the

defect levels [10]. The characteristics of dislocation contrast have been thoroughly studied in many works [10–12]. In particular, according to present-day understanding, the temperature dependence of the EBIC contrast can serve as an indicator of contamination of the dislocation with metal impurities [10, 13]. The parameters of the dislocation contrast are also found [14] to vary due to their interaction with oxygen, the common impurity in silicon.

Unlike the dislocations, the parameters of the EBIC contrast from dislocation trails have been measured in only a few works [7–9]. In particular, the temperature dependence of the trail contrast remains unknown, while such knowledge could clarify the nature of the trails. In the present work the EBIC contrast from dislocation trails was measured in the temperature range of 90–300 K in silicon samples with different impurity contents. To provide a direct comparison, the dislocation EBIC contrast was measured on the same samples. It is shown that the contrast of both dislocations and dislocation trails in p-Si increases with temperature while the opposite behaviour is observed in n-Si.

2. Experimental details

The experiments were carried out on p- and n-type samples doped with $\sim 10^{15}$ cm^{-3} boron and phosphorus atoms, respectively. Wafers with different oxygen concentration (grown by FZ and Cz techniques) were investigated. To check the effect of metal contamination, different deformation environments were used: one set-up was made of clean, semiconductor-grade ceramics; in the other one, the sample was in contact with steel. In a few cases the samples were contaminated with nickel.

The initial wafers were dislocation-free. After the damage resulting from the cutting procedure was removed by chemical etching, the dislocation sources were nucleated by scratching the (100) sample surface with a diamond tip. Then the samples were plastically deformed either in cantilever mode at 680 °C for 2 h or by four-point bending at 630 °C for 5 h. To reveal the deformation-induced defects, the (100) sample surface was selectively etched in Schimmel solution.

For the EBIC measurements, the Schottky barriers were formed on the chemically etched surface by thermal evaporation of Al or Au for p- and n-type samples, respectively. The EBIC measurements were carried out in the temperature range from 90 K to 300 K in a JSM-840A (Jeol) scanning electron microscope using a Keithley 428 current amplifier. Most measurements were carried out with beam energy $E_{\mathbf{b}} = 25$ keV and beam current $I_{\mathbf{b}} \sim 1 \times 10^{-10}$ A. As usual, the EBIC contrast of extended defects was determined as $C(\mathbf{r}) = 1 - I_{\mathbf{c}}(\mathbf{r})/I_{\mathbf{c0}}$, where $I_{\mathbf{c}}(\mathbf{r})$ and $I_{\mathbf{c0}}$ are the collected current values, measured with the focused e-beam located at a point $\mathbf{r}$ near the defect and far from it, respectively. To decrease data scattering and to account for the significant variations of the contrast value for different defects in the same sample, the same defects were used for measurements at different temperatures.

3. Results and discussion

Typical images in the EBIC and secondary electron (SE) modes of samples used in this study are shown in figure 1. The dark lines oriented along the ⟨110⟩ direction can be seen in the EBIC image (figure 1(a)). Comparison with the SE image (figure 1(b); the dislocation etch pits produce the dark contrast in the SE mode) shows that the dark lines in figure 1(a) correspond to positions where the moving dislocations intersect the sample surface [3]. The EBIC contrast is mainly determined by the dislocation trails rather than by dislocations. For example, the arrows labelled A in figure 1 point to positions where EBIC contrast is observed but no etch

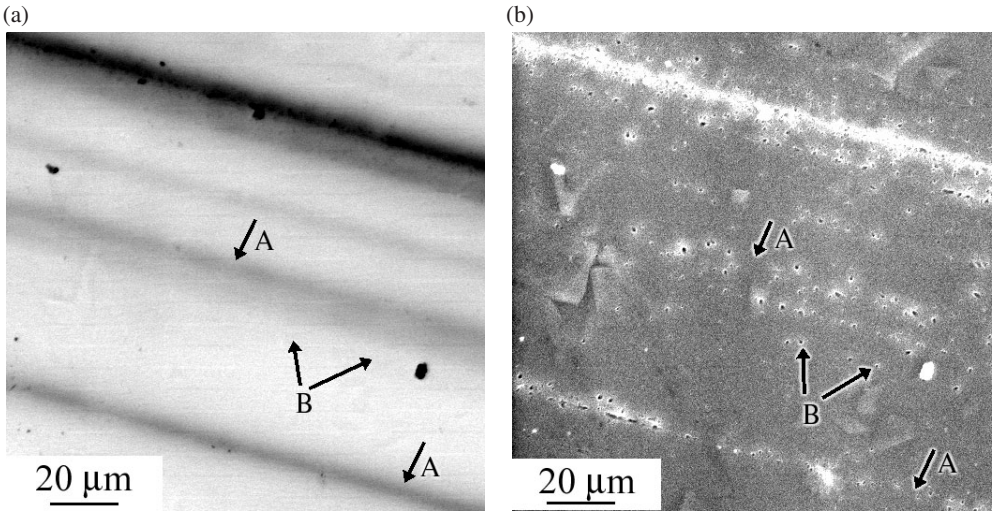

Figure 1. (a) EBIC and (b) SE images of FZ p-Si obtained at 300 K, $E_b = 25$ keV, $I_b = 1 \times 10^{-10}$ A.

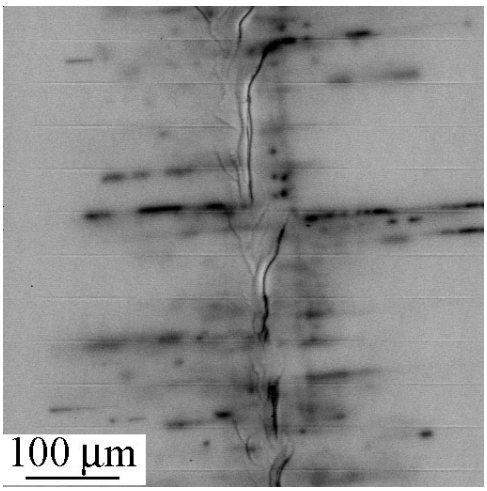

Figure 2. EBIC images of FZ p-Si obtained at 300 K, $E_b = 25$ keV, $I_b = 1 \times 10^{-10}$ A.

pits are revealed. In contrast, the arrows labelled B indicate the isolated dislocation etch pit, which produces no visible EBIC contrast.

Note that not all dislocations produce trails. For example, no detectable trail is associated with the dislocation indicated by the arrows labelled B. It looks as if the intensity of the trail signals is strongly dependent on the number of dislocations swept the given slip plane. This could explain the variations in the contrast of different trails. In some samples the EBIC contrast of the trails is observed to be inhomogeneous, showing multiple variations along the same slip plane. In figure 2, the scratch that served as a source of dislocations is located in the middle of the picture approximately vertically. It can be seen that the trail contrast consists of dark sections interspersed with regions of lighter contrast. The origin of such behaviour is still unknown.

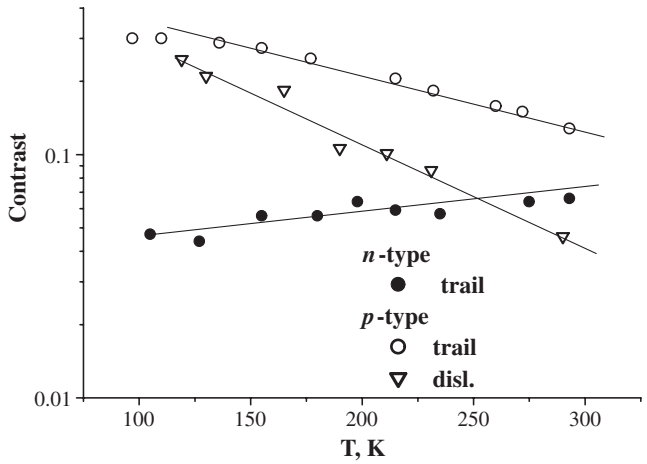

Figure 3. Temperature dependence of EBIC contrast of dislocations and dislocation trails in contaminated p-Si and dislocation trails in n-Si.

The temperature variations of the EBIC trail contrast are shown in figure 3. To exclude any influence of dislocations, the region without etch pits (see the arrows labelled A in figure 1) were used for the measurements. In n-type crystals, cooling the sample results in a decrease of the contrast. Although small, the decrease is observed in all n-type samples studied. In p-type crystals the EBIC contrast of the dislocation trails is increased by a factor of at least two due to the cooling down to 90 K. We believe that the opposite temperature trends observed for the n- and p-type samples reflect the asymmetry of the electronic structure of the defects located in the dislocation trails.

The EBIC contrast of dislocations was measured on those that were not associated with any trail. In most of the crystals the EBIC contrast of dislocations at room temperature is below the detection limit of $\sim$1% as seen in figure 1 under the arrows labelled B. The dislocation EBIC contrast in p-type crystals is found to increase due to metal contamination during the deformation procedure. The temperature dependence of the dislocation contrast measured on the contaminated sample is shown in figure 3 together with the data for dislocation trails. In those n-type samples where the dislocation EBIC contrast is above the detection limit, its value is rather small and decreases slightly with cooling. Neither the dislocations in n-type samples nor the dislocation trails in all crystals show any obvious correlation with the contamination level during deformation.

According to the classification of dislocation EBIC contrast on contamination level given in [10], the temperature dependence shown in figure 3 for the p-type sample can just about be considered to apply to the mixed type. At the same time, the dependence measured in n-type crystals cannot be classified in the scheme [10] because of the rather small contrast values observed and the similar contamination level expected. It should be mentioned in this connection that the asymmetry of the electronic properties of the dislocation has been established by different approaches. It is known that any crystals with moderate doping become p-type after plastic deformation to high dislocation density [15]. Moreover, an electrostatic barrier has been found around the individual dislocations and dense dislocations rows in n-type silicon [16], but has not been detected in p-type samples.

This study also found a strong effect of doping type on the EBIC contrast of dislocation trails (figure 3). The opposite temperature trends in n- and p-type silicon are similar to those for

the dislocation EBIC contrast in corresponding crystals. This can be interpreted as a similarity of the electronic properties of the defects located around dislocations and in dislocations trails, respectively. It could be mentioned in this connection that an electrostatic barrier has been found near the dislocation trails in n-type silicon [6].

4. Conclusion

The temperature dependences of the EBIC contrast of dislocations and dislocation trails have been measured in silicon crystals. It is found that temperature trends of the contrast are similar for both defects, but are opposite in n- and p-type samples. In p-type silicon the EBIC contrast decreases with temperature; this could be described by the Shockley–Read–Hall recombination model [17]. In n-type samples the slight increase of contrast with temperature is in qualitative accordance with the recombination governed by the electrostatic barrier.

Acknowledgment

The work was partly supported by the INTAS program (INTAS-01-0194).

References

[1] Alexander H and Teichler H 1991 *Mater. Sci. Technol.* **4** 249
[2] Steinman E A and Yakimov E B 1999 *Properties of Crystalline Silicon* ed R Hull (London: INSPEC) p 653
[3] Bondarenko I E *et al* 1981 *Phys. Status Solidi* a **68** 53
[4] Nikitenko V I, Farber B and Yakimov E B 1981 *Sov. Phys.—JETP Lett.* **34** 233
[5] Eremenko V, Abrosimov N V and Fedorov A 1999 *Phys. Status Solidi* a **171** 383
[6] Eremenko V G, Nikitenko V I and Yakimov E B 1978 *Sov. Phys.—JETP Lett.* **26** 65
[7] Aristov V V *et al* 1984 *Phys. Status Solidi* a **84** K43
[8] Yakimov E B, Bondarenko I E and Yarykin N 1986 *Mater. Sci. Forum* **10–12** 787
[9] Bondarenko I E *et al* 1986 *Phys. Status Solidi* a **95** 173
[10] Kittler M and Seifert W 1996 *Mater. Sci. Eng.* B **42** 8
[11] Alexander H 1994 *Mater. Sci. Eng.* B **24** 1
[12] Yakimov E B 1996 *Phys. Low-Dimens. Struct.* **1/2** 77
[13] Kveder V, Kittler M and Schröter W 2001 *Phys. Rev.* B **63** 115208
[14] Bondarenko I E and Yakimov E B 1990 *Phys. Status Solidi* a **122** 121
[15] Eremenko V G, Nikitenko V I and Yakimov E B 1978 *Sov. Phys.—JETP* **48** 598
[16] Eremenko V G, Nikitenko V I and Yakimov E B 1976 *Sov. Phys.—JETP* **42** 503
[17] Shockley W and Read W T 1952 *Phys. Rev.* **87** 835
Hall R N 1952 *Phys. Rev.* **86** 600